CARBON 54 (2013) 58–67

Available at www.sciencedirect.com

SciVerse ScienceDirect

journal homepage: www.elsevier.com/locate/carbon

Large scale atmospheric pressure chemical vapor deposition of graphene

Ivan Vlassiouk [a,*], *Pasquale Fulvio* [b], *Harry Meyer* [c], *Nick Lavrik* [d], *Sheng Dai* [b], *Panos Datskos* [a], *Sergei Smirnov* [e,f–5]

[a] *Measurement Science & System Engineering Division, Oak Ridge National Laboratory, Oak Ridge, TN 37831, USA*
[b] *Chemical Sciences Division, Oak Ridge National Laboratory, Oak Ridge, TN 37831, USA*
[c] *Materials Science and Technology Division, Oak Ridge National Laboratory, Oak Ridge, TN 37831, USA*
[d] *Center for Nanophase Materials Sciences, Oak Ridge National Laboratory, Oak Ridge, TN 37831, USA*
[e] *Department of Chemistry and Biochemistry, New Mexico State University, Las Cruces, NM 88003, USA*
[f] *NM Devices, LLC, 690 Canyon Point, Las Cruces, NM 88005, USA*

ARTICLE INFO

Article history:
Received 28 August 2012
Accepted 2 November 2012
Available online 23 November 2012

ABSTRACT

We demonstrate that large scale high quality graphene synthesis can be performed using atmospheric pressure chemical vapor deposition (CVD) on Cu and illustrate how this procedure eliminates major difficulties associated with the low pressure CVD approach while allowing straightforward expansion of this technology to the roll-to-roll industrial scale graphene production. The detailed recipes evaluating the effects of copper foil thicknesses, purity, morphology and crystallographic orientation on the graphene growth rates and the number of graphene layers were investigated and optimized. Various foil cleaning protocols and growth conditions were evaluated and optimized to be suitable for production of large scale single layer graphene that was subsequently transferred on transparent flexible polyethylene terephthalate (PET) polymer substrates. Such "ready to use" graphene–PET sandwich structures were as large as 40″ in diagonal and >98% single layer, sufficient for many commercial and research applications. Synthesized large graphene film consists of domains exceeding 100 μm. Some curious behavior of high temperature graphene etching by oxygen is described that allows convenient visualization of interdomain boundaries and internal stresses.

Published by Elsevier Ltd.

1. Introduction

Since the first recognized graphene isolation in 2004 by Novoselov et al. [1], this two dimensional material has become an intensive topic of fundamental and applied research. Great interest in graphene primarily arose due to its unique combination of remarkable properties including peculiar electronic band structure and very high charge carrier mobility [1–3], high optical transparency, flexibility, mechanical strength, electrical and thermal conductivities. All these qualities are promising for various applications in the areas spanning from electronics and composite structural materials to separation and desalination membranes, among many others. Despite of significant progress in the last few years, many of the proposed applications of graphene are still hampered either by technological difficulties in the production scale-up and integration into the multicomponent devices or require substantial research to prove their feasibility. One promising graphene application as a transparent electrode is arguably the closest to commercialization. Indeed, graphene is a very

* *Corresponding author.*
E-mail address: vlassioukiv@ornl.gov (I. Vlassiouk).
0008-6223/$ - see front matter Published by Elsevier Ltd.
http://dx.doi.org/10.1016/j.carbon.2012.11.003

attractive material for replacing indium tin oxide [4,5] in such applications as solar cells and touch screen displays. Rapidly growing worldwide demand for such products is affected by limited indium availability [6], as well as, environmental concerns and difficulties in ITO recycling [7], which makes the organic alternatives, such as graphene, increasingly important. Replacement of ITO and other conventional electrode materials by graphene requires adjustments that have been already addressed such as tuning the work function [8] and increasing conductance by doping [9]. Nevertheless, graphene synthesis at the industrial scale remains challenging and its development is imperative in shaping the technological fate of this material.

Although graphene of various qualities can be produced by different techniques [10–12], very few synthetic methods are economically viable and compatible with the currently available technological platforms. Chemical vapor deposition (CVD) approach for graphene growth [13–18] seems the most appealing because of its simplicity, scalability, large size of continuous graphene sheets, and reasonable material quality.

A possibility of graphene growth on metals [19] with negligible carbon solubility, particularly copper, was pointed out more than two decades ago [20]. More recently, a remarkable surge of interest in this approach was triggered by the seminal work published by the Ruoff's group [13]. However, the endeavor of optimizing CVD growth of graphene has revealed multiple challenges brought by the need of exploring an enormous experimental parameter space due to the multiple components involved. A vast majority of published results in this area has relied on reproducing the low pressure CVD recipe published in 2009.

Even though a low pressure CVD approach was shown to be scalable for large graphene film synthesis [14,21,22], it does not appear as appealing as the ambient pressure deposition for continuous high quality 'roll-to-roll' mass production of graphene. The challenges of such geometry include: feeding the catalyst foil into a low pressure reactor, severe evaporation of copper catalyst and requirement of a vacuum system compatible with flammable precursor gases. The last two aspects do not constitute major problems for a research oriented laboratory but they do translate into substantial obstacles for industrial scale graphene production and would contribute to increased production costs.

Atmospheric pressure CVD [23–26] is free of the aforementioned challenges and thus is more logical for applications in mass production. Its own hurdle, a nonuniform precursor distribution in the deposition chamber, can be overcome and, as we report here, large scale monolayer graphene sheets can be grown on Cu using atmospheric pressure CVD with the scale up to 40″. We also describe optimization of all technologically important steps, from the choice of foil, its pretreatment and graphene transfer onto flexible polymeric substrates.

2. Experimental

All chemical reagents of highest commercially available purity (from Aldrich) were used as received. Three types of Cu foils, from Alfa Aesar and from Nimrod Hall, were used, as described in Table 1.

2.1. Copper foil pretreatment used

(a) Soaking copper foils in acetone and isopropanol (IPA) was found insufficient to remove all organic contaminants. Thus, each side of the foil was wiped multiple times with paper tissues soaked in the corresponding solvents and then rinsed with IPA.
(b) Initially cleaned as in (a) samples were immersed in 1 M $FeCl_3$ solution in 3 M HCl for 10 min. The foils were then thoroughly washed with DI water and IPA.
(c) Initially cleaned as in (a) samples were electrochemically polished in 85% H_3PO_4 at 1.9 V using another copper sheet as a cathode until the current density dropped from ~20 mA/cm^2 to a value of about 10 mA/cm^2 (approximately 30–60 min). The foils were then thoroughly washed with DI water and IPA. Addition of polyethylene glycol (Sigma–Aldrich PEG, MW 400, 1:3 PEG:H_3PO_4) to increase viscosity of electropolishing solution that supposedly improves electropolishing procedure outcome [27] did not result in a noticeable decrease of surface roughness measured by optical profilometry.
(d) The treatments of initially cleaned as in (a) samples by immersion for 10 min either in 1 M HNO_3 solution or in 5 M acetic acid were also tried but proved to be unsatisfactory.

2.2. CVD

We used five zone 67″ long Thermocraft furnace equipped with a 6″ diameter quartz tube with air flow cooled flanges. The small (4″ × 4″) pieces of Cu foil were placed onto quartz plates, while large foil was wrapped onto the inner wall of the quartz tube. Graphene growth was performed as reported earlier [26], *i.e.* by sequential increase of the methane dosage that allows control of the number of graphene layers. The desired methane concentrations were achieved by mixing the flows of stock gases, 2.5% H_2 in Ar and 0.1% CH_4 in Ar (1000 ppm). Because of the low concentrations of both, H_2 or CH_4, the mixtures are nonflammable, which is an additional advantage of atmospheric CVD compared to the low pressure CVD. The total flow was kept at 5 L/min. Right before deposition each foil was first annealed for 1 h at 1000 °C in the hydrogen mixture and graphene was grown using a desired methane concentration (which can be varied in time) typically for 3 h. The optimal condition corresponded to stepwise increase of the methane concentration, 30, 50, 70, 100 ppm, for 45 min each. For incomplete coverage allowing visualization of individual hexagons, the growth was stopped after 90 min of synthesis. Right after the synthesis, the furnace was opened to allow cooling in 2.5% H_2 in Ar atmosphere, which typically took 1 h to reach room temperature.

2.3. Spectroscopy and analytical instrumentation

PHI 680 Scanning Auger Nanoprobe was used to obtain Auger data and Zeiss Merlin SEM for obtaining SEM images, Raman

Table 1 – Foils employed for graphene synthesis.

Sample name	Vendor/part number	Purity (%)	Thickness (μm)
AA1	Alfa Aesar, #13382	99.8	25
AA2	Alfa Aesar, #10950	99.999	25
NR	Nimrod Hall, #CR5	99.8	125

spectra were obtained on Renishaw instrument using 633 nm excitation.

To transfer graphene, the copper foil with graphene was laminated by a hot press Falcon 38″ laminator using 5 mil thick PET lamination film and the copper foil was dissolved in 1 M $FeCl_3$ solution in 3% HCl releasing the graphene on PET structure.

3. Results and discussion

3.1. *Foil preparation*

Quality of the CVD grown graphene is very much affected by the type and pretreatment of Cu catalyst foil [28,29] but not much details are given in the literature regarding its treatment prior to CVD. Different protocols can be compared for convenience, reproducibility and the outcome. We exclude from our consideration Cu films deposited on dielectric substrates [30] as they cannot be conveniently employed in the roll-to-roll production. Therefore, we focus on copper foils from the three representative commercially available sources characterized by different thickness and metal purity, from Alfa Aesar (AA1 and AA2) and from Nimrod Hall (NR), as described in Table 1.

The as received foils have surface contaminations (typically residual oils as well as some inorganic materials) originating from their manufacturing. Such contaminations cannot be entirely removed by commonly used acetone and alcohol cleaning, especially when dealing with large area foils. Incomplete elimination of the low vapor pressure oils from the catalyst can be one of the reasons for irreproducible rates of graphene growth reported in the literature, when graphene can appear even without an obvious carbon source [31]. Oil contaminations can be removed efficiently by mechanical scrubbing of metal surface with acetone and IPA soaked tissues.

Inorganic contaminants are not always removed this way and require more vigorous cleaning. Contaminations differ from sample to sample and can be removed with etching away thin layer of copper. Dipping in dilute HNO_3 solution does clean most of the foil surface except for small spots that remain visible in SEM, presumably at the points of attachment of bubbles that obstruct cleaning and also cause formation of pits on the copper surface.

Cleaning procedures that are not accompanied by gas evolution work much better. We tested the three protocols: redox reaction etching in an iron (III) chloride ($FeCl_3$) solution, electropolishing in phosphoric acid (H_3PO_4) [32,33], and "all-organic" treatment by acetic acid. Fig. 1a illustrates that electropolishing provides better result than cleaning by $FeCl_3$ – not only does it clean but also minimizes the surfaces roughness. The latter is important because graphene preferentially nucleates on surface irregularities, such as foil processing grooves [26] leading to a high density of graphene nucleation sites and, respectively, to small sizes of single crystal graphene domains. Large graphene domain sizes translate into higher mechanical strength and charge mobilities, which are the desired traits in graphene applications such as FET devices [34]. Nevertheless, graphene grown on either $FeCl_3$ treated or electropolished foil was of a similar quality. Our evaluation of graphene quality was based on measurements of graphene domain sizes, nucleation densities, and Raman spectra. In particular, intense 2D band ($I_{2D}/I_G \sim 3$) with the FWHM below 30 cm^{-1} (Fig. 1c), and the D band intensity below detection limit were found in both cases. Such criteria are consistent with high quality single layer graphene [35]. Treatment with acetic acid, on the other hand, did not produce as clean copper surface as in the previous two methods. Acetic acid readily dissolves copper oxide but does not etch copper metal, thus dissolution of copper oxide is not sufficient to clean all surface contaminants.

Fig. 1 shows SEM images of graphene grown on NR (b) and AA1 foils (c) for different pretreatments. The conditions for graphene growth on NR in Fig. 1b correspond to incomplete coverage (90 min growth time), which allowed visualization of separated domains. Distinct contaminations on graphene-free areas are clearly visible on untreated foils. The graphene domains (darker islands) show irregular shapes but with recognizable edges at 120° angles characteristic for samples prepared in hydrogen rich atmospheres [26]. Domains on the electropolished foil are regular hexagons of larger sizes (darker islands) and spread farther apart, *i.e.* the resulting graphene at full coverage will have fewer interdomain boundaries. Notably, graphene grown to full coverage on AA1 foil without additional treatment (Fig. 1c) demonstrates inferior quality.

We did not see a significant microscopic difference in the graphene quality grown on the foils pretreated using $FeCl_3$ and the electropolished ones despite a greater initial roughness for $FeCl_3$ treated foils. It is most likely due to severe copper surface reconstruction (mostly during annealing) at temperatures close to the melting point of copper. Intense surface reconstruction smoothes surface significantly and produces similarly low density of surface defects, such as kinks and atomic steps, which are the primary graphene nucleation sites, thus resulting in comparable nucleation densities for both pretreatment methods.

Copper vapor pressure increases significantly at high temperatures and reaches $P_{Cu} \sim 6.6 \times 10^{-3}$ Pa at 1000 °C [36] which translates into a very high vacuum evaporation rate of $Q_{vac} \sim 4$ μm/h [37] confirming the severe surface recon-

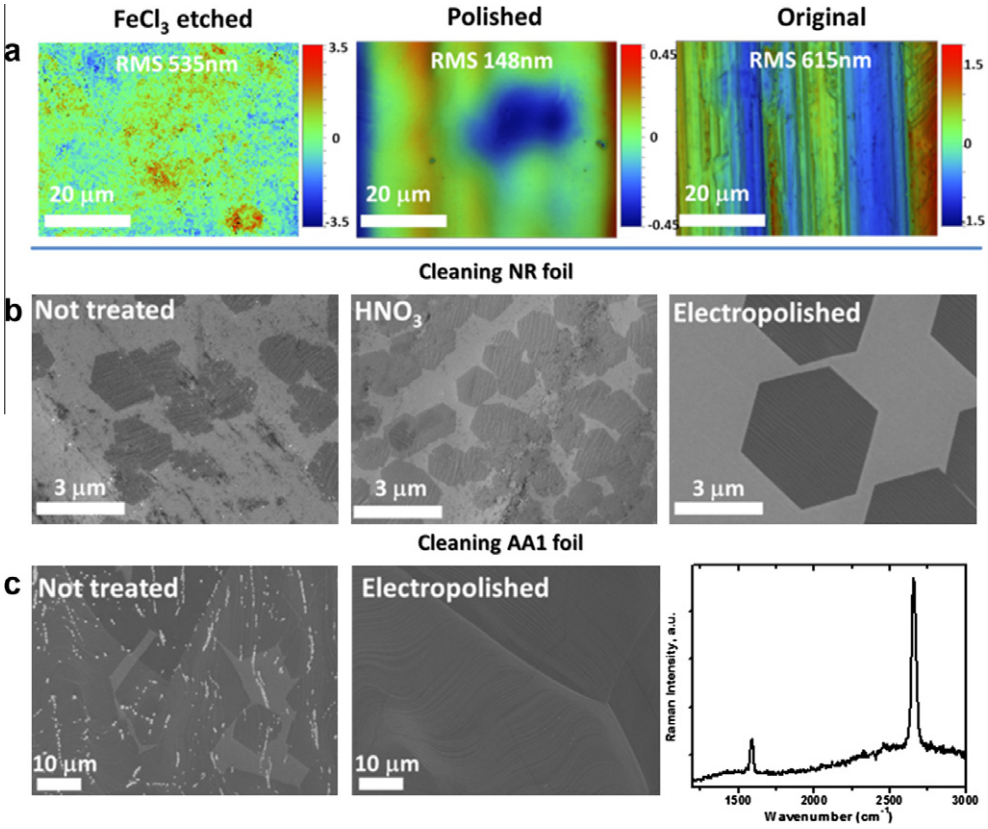

Fig. 1 – (a) Optical profilometry maps of the corresponding foils illustrating their roughness. Untreated AA1 sample shows the distinct processing grooves. Electropolished sample has the smoothest surface, however both cleaning procedures produce similarly good results for graphene growth. (b, c) SEM images of graphene on NR (b, partial coverage) and AA1 (c, almost 'full' coverage) commercial copper foils with different pretreatment procedures: not treated, cleaned by HNO_3 and electropolished. Characteristic Raman spectra of graphene grown on electropolished foil shown in (c). Cleaning by $FeCl_3$ results in similar to that of electropolished foil. See text for details.

struction. At ambient pressure, the evaporation rate drastically decreases (inversely proportional to the pressure) [38] which is confirmed by almost no copper deposits in the atmospheric CVD tube and it presents a significant advantage of the atmospheric pressure protocol over the low pressure CVD for graphene synthesis. According to [37], the rate of copper atoms evaporation at atmospheric pressure is at least three orders of magnitude less than in vacuum.

The residues of $FeCl_3$ are present on copper after its treatment by iron chloride even after thorough washing in DI water. Fortunately, $FeCl_2$ and CuCl are much more volatile than Cu itself resulting in recognizable deposits of white anhydrous $FeCl_2$ along the quartz tube outside of the heating zone. It also positively contributes to the copper surface reconstruction. The chlorine reappears on Cu regions not covered by graphene, as identified by Auger electron spectroscopy (AES) in Fig. 2, most likely during cooling when graphene deposition stops.

Electropolishing in phosphoric acid results in the foils with the smoothest surfaces that do not produce deposits of white anhydrous $FeCl_2$ on the tube when heated and very little of phosphor contamination arises on the graphene covered copper. Thus electropolishing appears to be the best choice for foil pretreatment for large scale graphene synthesis, which we primarily have used, unless it is stated otherwise.

3.2. *Graphene growth*

In both roll-to-roll and batch mode production, the synthesized graphene is eventually exposed to the atmosphere. Based on the Raman spectroscopy results, graphene not only withstands oxidation under ambient atmosphere and temperatures as high as 400 °C but it also protects Cu from oxidation by oxygen or chlorine. Thus, complete furnace cooling to a room temperature is not required allowing significant acceleration of the overall graphene synthesis procedure. Graphene capability to serve as a very effective corrosion resistant layer [39–41] has been confirmed by AES for a sample exposed to air at 300 °C, that exhibits negligible amounts of oxygen in the areas covered by graphene in comparison to bare copper (Fig. 2 and Table 2).

The O/Cu ratio on regions covered by graphene (0.05 ± 0.02) is more than an order of magnitude smaller than on bare copper (0.8 ± 0.01). Graphene double layers [42] in the center of some individual crystals are clearly distinguished by AES due to larger carbon content and can be seen as red areas in

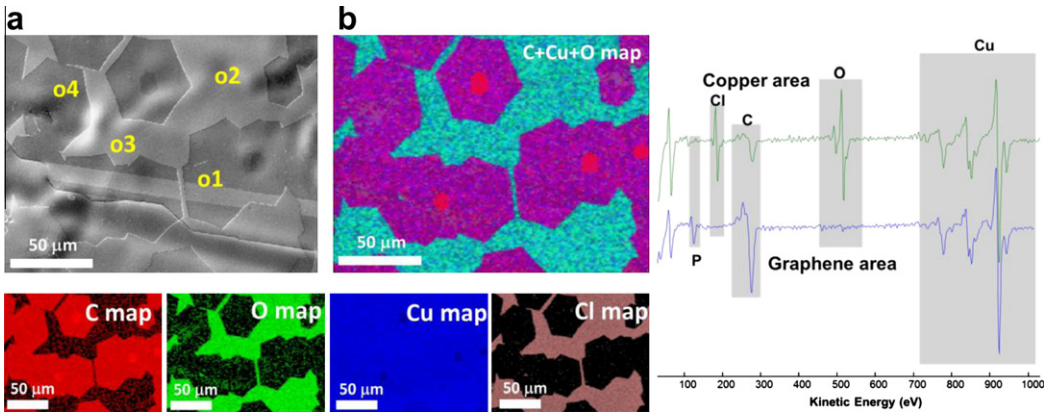

Fig. 2 – Auger spectroscopy surface analysis (• C • O • Cu • Cl) of graphene on Cu. Graphene is stable in ambient environment up to 400 °C and can be used as corrosion resistant protective layer which is clearly demonstrated by a low oxygen peak under graphene after sample oxidation at 300 °C. Graphene bilayer is clearly seen in AES as red areas in b due to larger carbon content. (For interpretation of the references to color in this figure legend, the reader is referred to the web version of this article.)

Table 2 – Surface composition (at.%) after individual graphene domain growth and oxidation for AES map shown in Fig. 3.

Area in Fig. 2	C (%)	O (%)	Cu (%)	Cl (%)	P (%)	O/Cu
1	74.9	0.6	23.4	0	1.1	0.03
2	25.8	31.9	39.6	2.7	0	0.81
3	57.1	1.8	37.9	0	3.2	0.05
4	23.5	32.5	41.2	2.7	0	0.79

Fig. 2b. Note that for the successful commercialization of graphene, a rapid turnaround of the foils and consequent exposure of hot samples to air may be necessary since complete cooling of our 96″ long, 5 heating zones, 6″ tube furnace to room temperature would require 12 h or more. Hence, the AES results indicate that the synthesis time can be greatly shortened. Exposure of graphene to air at higher temperatures induces its etching and thus should be avoided (Fig. 3). The etching starts at the interdomain boundaries and clearly visualizes them. It further expands into each domain in a dendritic-like etching pattern leaving diagonal stripes etch-free. The mechanism of this pattern formation is not certain but it likely proceeds along the stress induced ripples [43] on the graphene domain. It has no apparent correlation with the Cu surface orientation – the pattern does not change when crossing Cu domain boundaries in Fig. 3b. Note also that a similar conformal etching pattern appears on the top layer graphene (Fig. 3d). This technique allows visualization of graphene domains and shows that in our large films they are as large as tenths of a millimeter. This etching pattern is very different from etching by nanoparticles, where it proceeds along zigzag lines and produces hexagonally shaped holes [26] in otherwise continuous graphene.

The rate of graphene growth is of major importance in its commercialization. The growth rate depends not only on the copper foil pretreatment but also on the copper purity and crystallographic orientation of the copper domains and thus requires individual optimization for each case. Fig. 4a shows that NR foils have lower graphene coverage compared to AA1 sample grown under the same conditions. Given their similar 99.8% copper content and equal foil roughness achieved by electropolishing procedure, the nucleation densities of graphene should be similar but the rate of further growth is obviously different, with some preference for AA1. The two other properties, apart from copper purity, distinguishing Cu substrates are the thickness and the domain orientations. The two might be related but we do not have unambiguous means for evaluating the effect of thickness separately – similar metal purity AA1 and NR foils are from different sources. It is unlikely that the foil thickness plays a defining role since the deposition temperatures are near the melting point of Cu substrate and the possible stresses induced by graphene overlayer should be readily released. Small differences in the amount of hydrogen dissolved in substrates of different thickness should not be of critical importance either since the synthesis is performed in hydrogen rich environment. More important are the surface crystallographic orientations which differ between AA and NR foils. According to XRD shown in Fig. 4a, annealed AA1 has almost exclusively ⟨100⟩ orientation while NR is a mix of ⟨111⟩ with the other facets of higher indices. Crystallographic orientation of the catalyst foil affects several core processes involved in graphene growth including the carbon precursor dehydrogenation [44] and adsorption, [48] generation of hydrogen atoms [45,46], and surface diffusion [47]. Based on current results, it is not possible to delineate each of these effects but overall growth on ⟨100⟩ (AA foils) is faster compared to ⟨111⟩ (NR foils) at ambient pressures, which is not the case for low pressure synthesis and lower synthesis temperature, where ⟨111⟩ was reported to be the fastest [49].

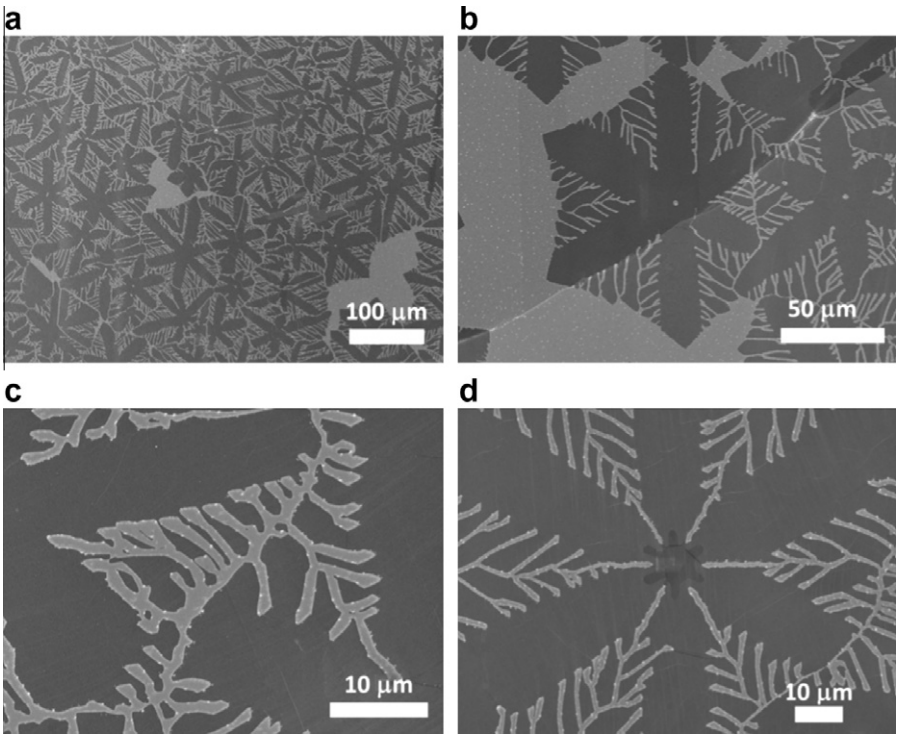

Fig. 3 – SEM images of graphene on polished NR foil etched by oxygen when the CVD furnace was opened to air at high temperature >400 °C. Oxidation starts at the interdomain boundaries (which clearly visualizes them) and evolves into a dendritic-like etching pattern that likely proceeds along the stress induced ripples on each graphene grain. Note that a similar conformal etching pattern appears on the top layer graphene (d).

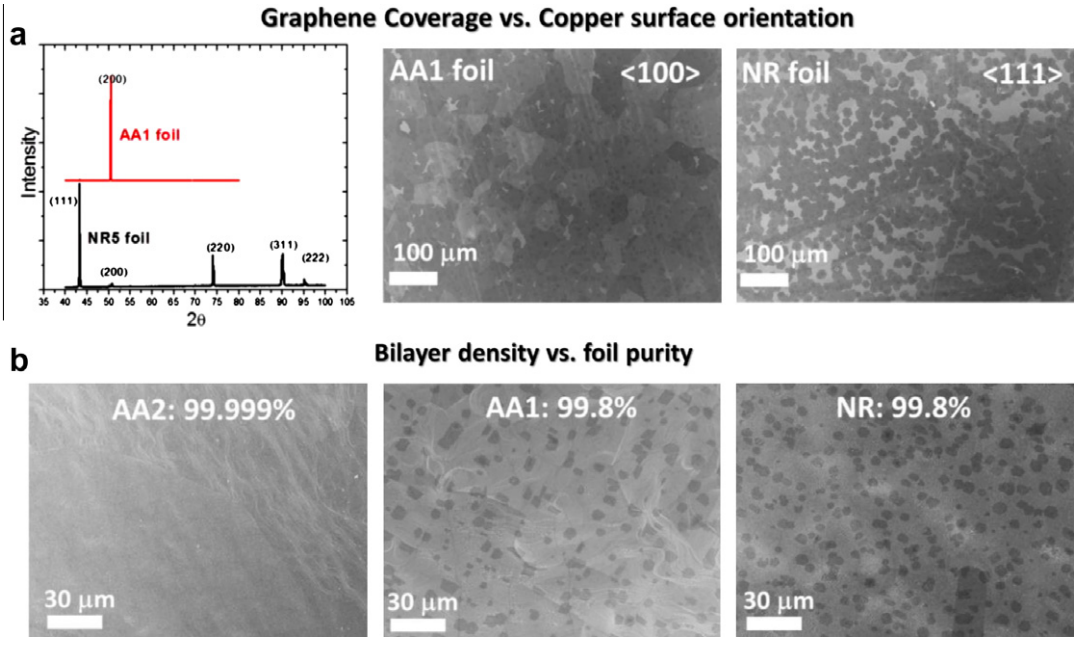

Fig. 4 – (a) SEM images illustrate a higher graphene growth rate on polished AA1 than on polished NR foil at the same conditions. XRD of annealed AA1 shows exclusively ⟨100⟩ orientation, while NR foil has mostly ⟨111⟩ with smaller contributions from ⟨110⟩ and ⟨311⟩. The copper domains are much larger for NR foils. (b) Effect of impurities in Cu on the density of bilayers. Full coverage graphene layer on: AA2, AA1 and NR grown at slightly higher than typical methane concentration shows that only the purest foil AA2 (99.999%) has almost no double layers.

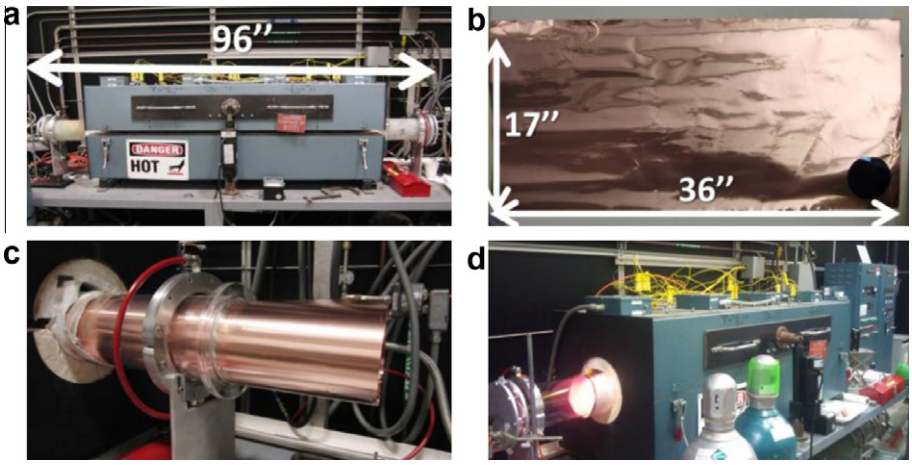

Fig. 5 – ORNL setup for 36″ × 17″ monolayer graphene growth using atmospheric pressure CVD. (a) 5 zone furnace with 96″ long 6″ diameter quartz tube. (b) NR copper foil, 4″ wafer is shown for comparison. (c) Copper foil from B loaded into the quartz tube. (d) The setup during atmospheric pressure CVD synthesis of graphene at 1000 °C.

More important is the effect of metal purity. Fig. 4b shows that graphene grown under the same conditions on all three foils of identical pretreatment also demonstrate different amounts of multilayers. It illustrates that the optimal conditions for perfect coverage and minimal contribution of multilayers are not the same for these foils. The 99.999% purity AA2 foil has almost exclusively single layer graphene, while significant amounts of bilayers are observed on 99.8% AA1 and NR foils Thus even a small rise in the amount of impurities in AA1 and NR foils significantly increases the rate of multilayer graphene formation. To determine the nature of impurities (with Ni being one of likely 'culprit') and explain their effect on graphene growth require more thorough investigation. That role may include a greater catalytic activity for carbon activation, an increased solubility of carbon in the substrate or a more efficient surface defect for the graphene seed growth under oversaturation with active carbon species. Nevertheless, the optimal conditions for AA1 and NR foils adjusted to have a lower concentration of methane also produce high quality graphene with >99% monolayer coverage. The optimal conditions also depend on temperature of synthesis and the furnace dimensions, as well as, on the chosen flow rates and concentrations of gases and even on the foil size. Below we outline how these optimal conditions can be narrowed down for methane gas as a carbon source but note that other carbon sources can be similarly optimized as well. For example, similar high quality graphene requires significantly lower partial pressure of ethane.

Fig. 5 presents a photograph of our setup based on a five zone 67″ long furnace equipped with a 6″ diameter quartz tube with air flow cooled flanges. Optimization of graphene growth on large foils is particularly challenging and thus is appropriate for pinpointing the crucial features in that procedure. We chose NR foil because of its low cost and larger thickness, which makes its handling much easier and can be applied for synthesis of large area (17″ × 36″) single layer graphene. Right before deposition, the foil was annealed for 1 h at 1000 °C in the hydrogen mixture (2.5% H_2 in Ar at 5 L/min) and the optimized conditions were used to deposit single layer graphene. The deposition temperature affects both the density of seeds and the growth rate; the chosen 1000 °C is far enough from the melting temperature of copper and thus is convenient for handling large size foils. At the same time, high quality of graphene can be grown at this temperature [26].

As we have demonstrated before [26], the role of hydrogen is dual: it serves as a cocatalyst activating adsorbed methane and as an etchant that eliminates dangling bonds (and probably contributes to the density of seeds). As a result, the rate of graphene growth has a maximum as a function of the ratio between the hydrogen and methane concentrations (H_2/$CH_4 \sim 300$ at 1000 °C). Because the amount of activated carbon is also proportional to the surface area of copper not covered with graphene, the highest concentration of activated carbon is at the beginning and, if not kept low enough, can result in production of multilayers. Because the activated carbon concentration decreases with increasing graphene coverage, the rate of multilayer production dramatically drops with time but so does the overall rate of growth as well. With a low enough density of separated graphene domains, this scenario leads to the eventual terminal size of the domains and thus to incomplete coverage. When the density of graphene seeds is high (e.g., due to poor quality of surface cleaning or low deposition temperature), both problems can never materialize but the resulting graphene would have small domains and thus inferior mechanical, electrical and thermal properties [17]. As was previously demonstrated [26], gradual increase of the methane concentration circumvents the problems associated with changing the rate of activated carbon production. For our experimental conditions described above, the optimum was achieved using a sequence of 30, 50, 70, 100 ppm methane concentrations added to the hydrogen mixture for 45 min each.

Graphene growth on a large foil further exaggerates the above mentioned problems. Due to the large tube volume, the gas flow rates have to be very high to equilibrate the

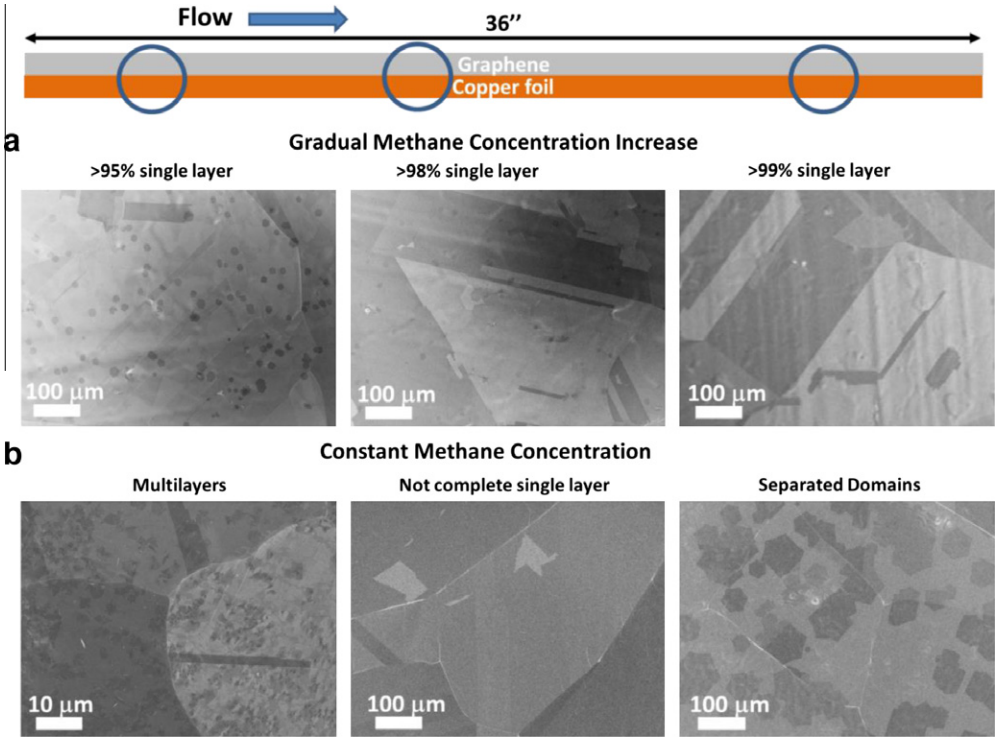

Fig. 6 – Evaluation of the graphene quality at various distances along the CVD tube for atmospheric pressure CVD. The carbon precursor (methane) concentration rises faster at the inlet resulting in a greater abundance of multilayers seen as darker islands. (a) Gradual methane concentration increase allows mostly single layer graphene growth over all 36″ length under atmospheric pressure conditions. (b) Constant methane concentration yields high percentage of multilayers on the inlet, incomplete coverage in the middle (empty areas are lighter voids) and separated single domains (darker islands) at the outlet due to large methane concentration gradient.

methane concentration along the entire length of the tube within a short period of time. One can find a trade-off optimum of not too high rates to minimize the cost but it means that the gas concentrations vary along the tube. For the present geometry, flow rates of 5 L/min equate the Reynolds number $Re < 10$,[1] corresponding to a laminar regime. In the simplest approximation – the plug flow model – it corresponds to approximately 20 min needed to replace the gas volume in the tube. Thus, the foil near the tube inlet is effectively exposed longer to the $CH_4/H_2/Ar$ mixture compared to the portion near the outlet. Moreover, since a significant portion of methane is consumed along the way, the flow front smears beyond diffusion and the methane concentration near the outlet increases even slower. Thus, the primary purpose of gradual increase of the methane concentration during synthesis is to minimize the growth of bilayers at the inlet and the total duration of the synthesis, as well as the highest methane concentration, should be chosen to ensure complete coverage near the outlet. The optimization is performed by focusing on these two indicators and is a bit more restrictive than optimization on a small foil placed at a certain position in the furnace.

Fig. 6a illustrates the graphene quality for near the optimum conditions for the largest foil (17″ × 36″), where only single layer coverage (and large crystal sizes) is observed near the end of the tube reactor and less than 5% of bilayers (darker spots) are seen near the inlet. The overall bilayer coverage does not exceed 2%. Note that the total coverage is close to 100% on both ends. As shown in Fig. 6b, maintaining constant methane concentration during synthesis produces inferior results. Using 60 ppm of methane for 3 h deposition, instead of even portions of 30, 50, 70, 100 ppm (45 min long each), results in increasing contribution of graphene multilayers at the inlet, while the coverage at the outlet is incomplete, with visible separated graphene domains. Low pressure CVD does not have the complication of uneven precursor concentration even in a large tube, due to much faster diffusion. Nevertheless, gradual increase of methane concentration in atmospheric pressure CVD [26] circumvents the problem and allows growing almost exclusively single layer graphene over large areas, as is demonstrated by SEM in Fig. 6a and confirmed by Raman spectra. Further lowering of the initial methane concentration (below 30 ppm) totally eliminates double layers even at the inlet.

Thicker than typically used copper foil (125 μm) was found necessary for large scale graphene production not only for convenience of pretreatment and sufficient rigidity during high temperature deposition but also for its handiness during

[1] Reynolds number is calculated based on the Ar density, $\rho = 0.265$ kg/m^3 and the dynamic viscosity, $\mu = 5.2 \times 10^{-5}$ kg/ms at 1000 °C, the flow velocity, $u = 4.4 \times 10^{-3}$ m/s, and the tube diameter, $D = 0.15$ m, $Re = \rho uD/\mu \sim 3$.

Fig. 7 – Transfer of graphene films on flexible, transparent PET polymer: lamination of copper foil with graphene by PET polymer; laminated sample, 4″ wafer is shown for comparison; Example of 40″ graphene film on PET polymer prepared by atmospheric pressure CVD synthesis with sheet resistance 1–3 kΩ/sq.

post deposition. One-step approach using a lamination machine to coat the synthesized graphene with PET polymer can be employed (Fig. 7) for graphene transfer of such large scale. It is followed by the standard dissolution of the copper foil by $FeCl_3$. As Fig. 7 shows, we have succeeded in producing transparent 40″ in diagonal PET–graphene films. The final sheet resistance of these "ready to use" films was 1-3kΩ/sq., which is similar to smaller samples reported in the literature [4] making this approach attractive for further applications requiring transparent conducting electrode materials. The resistance can be further minimized by chemical doping methods reported in the literature [8].

4. Conclusions

Protocols allowing a high quality (with domains >100 μm) large scale (up to 40″ in diagonal) graphene growth using atmospheric pressure chemical vapor deposition on copper foils were elucidated in details, from the foils pretreatment to graphene transfer onto PET polymer. Copper foil pretreatment by electropolishing in H_3PO_4 or redox etching by $FeCl_3$ was found to result in superior quality of graphene when compared with no treatment or with etching of the foils by nitric or acetic acids. Electropolishing appears more convenient as a catalyst pretreatment method because it produces the least contamination and the minimal roughness.

Copper foils purity and the crystallographic orientation influence the graphene growth rate and the density of seeds defining the size of graphene domains: the ⟨111⟩ orientation (NR foils) appears to have a lower growth rate than ⟨100⟩ (AA foils), and the highest copper purity (99.999%) has a slower rate than the less expensive foils with 99.8% purity. For each choice of foil, an optimal protocol for producing almost exclusively single layer graphene (>98%) over a large area (beyond 4×10^3 cm^2) can be identified. In an optimized protocol, the methane concentration (in its mixture with hydrogen and argon) is gradually increased during synthesis to minimize the contribution of bilayers by lowering the initial methane concentration and to ensure the complete coverage over the whole surface area by extending the deposition time at the highest methane concentration. The foil thickness does not seem to play a defining role in the growth process but thicker foils are more practical in the large scale synthesis due to the ease of handling.

Graphene is stable in air up to 400 °C and even serves as an effective corrosion resistant layer for Cu; shortening of the cooling time before reaching the room temperature can be advantageous for commercial synthesis. Exposure to oxygen at higher temperatures results in nonuniform etching by oxygen, in which individual graphene domains can be visualized. An interesting dendritic-like pattern of etching developing along the internal stresses in graphene is observed for the first time.

A shortened protocol for large area graphene direct transfer from Cu foils onto polymer using commercially available lamination machine was introduced and was realized in the "ready to use" graphene–PET structures as large as 40″ having graphene domains generally larger than 100 μm. Due to its convenience, the method can be employed in a wide range of applications.

Acknowledgements

I.V. was supported by the Laboratory Directed Research and Development Program of Oak Ridge National Laboratory (ORNL), managed by UT-Battelle, LLC for the US Department of Energy under Contract No. DEAC05-00OR22725. Authors thank Dr. K. Xia and Dr. M. Regmi for valuable help in obtaining XRD data; I. Ivanov for help with Raman characterization; Charles Schaich and Jim Kiggans for technical assistance. A portion of this research was conducted at the Center for Nanophase Materials Sciences, which is sponsored at Oak Ridge National Laboratory by the Scientific User Facilities Division, Office of Basic Energy Sciences, US Department of Energy.

REFERENCES

[1] Novoselov KS, Geim AK, Morozov SV, Jiang D, Zhang Y, Dubonos SV, et al. Electric field effect in atomically thin carbon films. Science 2004;306:666–9.
[2] Geim AK, Novoselov KS. The rise of graphene. Nat Mater 2007;6:183–97.
[3] Geim AK. Graphene: status and prospects. Science 2009;324:1530–4.
[4] Li X, Zhu Y, Cai W, Borysiak M, Han B, Chen D, et al. Transfer of large-area graphene films for high-performance transparent conductive electrodes. Nano Lett 2009;9:4359–63.
[5] Zhu Y, Sun Z, Yan Z, Jin Z, Tour JM. Rational design of hybrid graphene films for high-performance transparent electrodes. ACS Nano 2011;5:6472–9.
[6] Report on Critical materials atrategy. US Department of Energy, 2010.
[7] Li J, Gao S, Duan H, Liu L. Recovery of valuable materials from waste liquid crystal display panel. Waste Manag 2009;29:2033–9.

[8] Shi Y, Kim K, Reina A, Hofmann M, Li L-J, Kong J. Work function engineering of graphene electrode via chemical doping. ACS Nano 2010;4:2689–94.
[9] Wei D, Liu Y, Wang Y, Zhang H, Huang L, Yu G. Synthesis of N-doped graphene by chemical vapor deposition and its electrical properties. Nano Lett 2009;9:1752–8.
[10] Forbeaux I, Themlin J-M, Debever J-M. Heteroepitaxial graphite on 6H–SiC(0001): interface formation through conduction-band electronic structure. Phys Rev B 1998;58:16396–406.
[11] Hass J, Marchenkov AN, Conrad EH, First PN, de Heer WA. Electronic confinement and coherence in patterned epitaxial graphene. Science 2006;312:1191–6.
[12] Zhu Y, Murali S, Cai W, Li X, Suk JW, Potts JP, et al. Graphene and graphene oxide: synthesis properties and applications. Adv Mater 2010;22:3906–24.
[13] Li X, Cai W, An J, Kim S, Nah J, Yang D, et al. Large-area synthesis of high-quality and uniform graphene films on copper foils. Science 2009;324:1312–4.
[14] Bae S, Kim H, Lee Y, Xu X, Park J-S, Zheng Y, et al. Roll-to-roll production of 30-inch graphene films for transparent electrodes. Nat Nanotechnol 2010;5:574–8.
[15] Reina A, Jia X, Ho K, Nezich D, Son H, Bulovic V, et al. Large area, few-layer graphene films on arbitrary substrates by chemical vapor deposition. Nano Lett 2009;9:30–5.
[16] Yu Q, Lian J, Siriponglert S, Li H, Chen Y, Pei S-S. Graphene segregated on Ni surfaces and transferred to insulators. Appl Phys Lett 2008;93:113103.
[17] Vlassiouk I, Smirnov S, Ivanov I, Fulvio P, Dai S, Meyer H, et al. Electrical and thermal conductivity of low temperature CVD graphene: the effect of disorder. Nanotechnology 2011;22:275716.
[18] Ruan G, Sun Z, Peng Z, Tour JM. Growth of graphene from food, insects, and waste. ACS Nano 2011;5:7601–7.
[19] Oshimayx C, Nagashim A. Ultra-thin epitaxial films of graphite and hexagonal boron nitride on solid surface. J Phys Condens Matter 1997;9:1–20.
[20] Alstrup I, Chorkendorff I, Ullman S. The interaction of CH_4 at high temperatures with clean and oxygen precovered Cu(100). Surf Sci 1992;264:95–102.
[21] Han GH, Shin H-J, Kim ES, Chae SJ, Choi J-Y, Lee YH. Poly(ethelene co-vinyl acetate)-assisted one-step transfer of ultra-large graphene. Nano 2011;6:59–65.
[22] Yamada T, Ishihara M, Kim J, Hasegawa M, Iijima S. A roll-to-roll microwave plasma chemical vapor deposition process for the production of 294 mm width graphene films at low temperature. Carbon 2012;50:2615–9.
[23] Bhaviripudi S, Jia X, Dresselhaus MS, Kong J. Role of kinetic factors in chemical vapor deposition synthesis of uniform large area graphene using copper catalyst. Nano Lett 2010;10:4128–33.
[24] Robertson A, Warner JH. Hexagonal single crystal domains of few layer graphene on copper foils. Nano Lett 2011;11:1182–9.
[25] Yu Q, Jauregui LA, Wu W, Colby R, Tian J, Su Z, et al. Control and characterization of individual grains and grain boundaries in graphene grown by chemical vapour deposition. Nat Mater 2011;10:443–9.
[26] Vlassiouk I, Regmi M, Fulvio P, Dai S, Datskos P, Eres G, et al. Role of hydrogen in chemical vapor deposition growth of large single-crystal graphene. ACS Nano 2011;5:6069–76.
[27] Landolt D. fundamental aspects of electropolishing. Electrochem Acta 1987;32(1):11.
[28] Luo Z, Lu Y, Singer DW, Berck ME, Somers LA, Goldsmith BR, et al. Effect of substrate roughness and feedstock concentration on growth of wafer-scale graphene at atmospheric pressure. Chem Mater 2011;23:1441.
[29] Han GH, Gunes F, Bae JJ, Kim ES, Chae SJ, Shin H-J, et al. Influence of copper morphology in forming nucleation seeds for graphene growth. Nano Lett 2011;11:1444–7.
[30] Levendorf MP, Ruiz-Vargas CS, Garg S, Park J. Transfer-free batch fabrication of single layer graphene transistors. Nano Lett 2009;9:4479–83.
[31] Pollard AJ, Nair RR, Sabki SN, Staddon CR, Perdigao LMA, Hsu CH, et al. Formation of monolayer graphene by annealing sacrificial nickel thin films. J Phys Chem C 2009;113:16565–7.
[32] Van Gils S, Le Pen C, Hubin A, Terryn H, Stijnsb E. Electropolishing of copper in H_3PO_4 ex situ and in situ optical characterization. J Electrochem Soc 2007;154:C175–80.
[33] Shivareddy S, Bae S, Brankovic S. Cu surface morphology evolution during electropolishing. Electrochem Solid State Lett 2008;11:D13–7.
[34] Li X, Magnuson CW, Venugopal A, An J, Suk JW, Han B, et al. Graphene films with large domain size by a two-step chemical vapor deposition process. Nano Lett 2010;10:4328–34.
[35] Ferrari AC. Raman spectroscopy of graphene and graphite: disorder, electron–phonon coupling, doping and nonadiabatic effects. Solid State Commun 2007;143(47):57.
[36] Hersh H. The vapor pressure of copper. J Am Chem Soc 1953;75:1529–31.
[37] Melmed AJ, Keating KB. On the evaporation of high-purity copper in hydrogen. Surf Sci 1966;5:166–9.
[38] Fonda GR. Evaporation of tungsten under various pressures of argon. Phys Rev 1928;31:260–6.
[39] Chen S, Brown L, Levendorf M, Cai W, Ju S-Y, Edgeworth J, et al. Oxidation resistance of graphene-coated Cu and Cu/Ni alloy. ACS Nano 2011;5:1321–7.
[40] Prasai D, Tuberquia JC, Harl RR, Jennings GK, Bolotin KI. Graphene: corrosion-inhibiting coating. ACS Nano 2012;6:1102–8.
[41] Raman RKS, Banerjee PC, Lobo DE, Gullapalli H, Sumandasa M, Kumar A, et al. Protecting copper from electrochemical degradation by graphene coating. Carbon 2012;50:4040–5.
[42] Kalbac M, Frank O, Kavan L. The control of graphene double-layer formation in coppercatalyzed chemical vapor deposition. Carbon 2012;50:3682–7.
[43] Bao W, Miao F, Chen Z, Zhang H, Jang W, Dames C, et al. Controlled ripple texturing of suspended graphene and ultrathin graphite membranes. Nat Nanotechnol 2009;4:562–6.
[44] Zhang W, Wu P, Li Z, Yang J. First-principles thermodynamics of graphene growth on Cu surfaces. J Phys Chem C 2011;115:17782–7.
[45] Gelb A, Cardillo M. Classical trajectory studies of hydrogen dissociation on a Cu(100). Surf Sci 1976;59:128–40.
[46] Gelb A, Cardillo M. Classical trajectory study of the dissociation of hydrogen on copper single crystals. II. Cu(100) and Cu(110). Surf Sci 1977;64:197–208.
[47] Fan L, Zou J, Li Z, Li X, Wang K, Wei J, et al. Topology evolution of graphene in chemical vapor deposition, a combined theoretical/experimental approach toward shape control of graphene domains. Nanotechnology 2012;23:115605.
[48] Pang X-Y, Xue L-Q, Wang G-C. Adsorption of atoms on cu surfaces: a density functional theory study. Langmuir 2007;23:4910–7.
[49] Wood JD, Schmucker SW, Lyons AS, Pop E, Lyding JW. Effects of polycrystalline cu substrate on graphene growth by chemical vapor deposition. Nano Lett 2011;11:4547–54.